Asymmetric Fraunhofer Spectra in a Topological Insulator-Based Josephson Junction

Alexander Beach, Dalmau Reig-i-Plessis, Gregory MacDougall, Nadya Mason

Department of Physics and Materials Research Laboratory, University of Illinois, Urbana 61801 IL, United States

E-mail: arbeach2@illinois.edu, nadya@illinois.edu

Abstract

Josephson junctions with topological insulators as their weak link (S-TI-S junctions) are predicted to host Majorana fermions, which are key to creating qubits for topologically protected quantum computing. But the details of the S-TI-S current-phase relation and its interplay with magnetic fields are not well understood. We fabricate a Bi_2Se_3 junction with NbTi leads and measure the Fraunhofer patterns of the junction with applied in-plane fields. We observe that asymmetric Fraunhofer patterns appear in the resistance maps of B_z vs. $B_{x,y}$, with aperiodic node spacings. These asymmetric patterns appear even at zero parallel field and for temperatures up to 1 K. The anomalous features are compared to asymmetric Fraunhofer patterns expected for finite Cooper pair momentum shifts as well as geometric effects. We show that the geometric effects can dominate, independent of in-plane field magnitude. These results are important for differentiating geometrical phase shifts from those caused by Cooper pair momentum shifting, Majorana mode signatures, or other unconventional superconducting behavior.

1. Introduction

Josephson junctions are integral to the ultra-sensitive detection of magnetic fields via SQUIDs, and the construction of superconducting qubits [1]. A standard Josephson junction obeys the Josephson equations, $I_c = I_{c,0} \sin(\Delta \varphi)$ and $V = \sim 2e - \partial(\Delta \varphi) \partial t$, where $\Delta \varphi$ is the phase difference between the contacts of the junction, and $I_{c,0}$ is the critical current of the junction in the absence of a magnetic field. Thus the phase difference across a Josephson junction is tied to much of the essential physics of a device, including the critical current, voltage across the junction, and pairing symmetry.

For a standard Josephson junction, the phase difference across the junction is zero when there is no current across it. However, it is known that by breaking combinations of spatial parity and time reversal symmetries, there should be an anomalous current across the junction at $\Delta \varphi = 0$ [2]. In particular, as described in Ref. [3], specific combinations of magnetic fields and disorder potentials can lead to anomalous phase shifts.

For example, the combination of an applied field parallel to the direction of the current, high spin-orbit coupling, and a disorder potential in the direction of the current, are enough to cause an anomalous phase shift. In this manuscript we discuss anomalous phase shifts due to the combination of spin-orbit coupling, sample disorder, and applied fields both in and out of the plane of the junction.

Josephson junctions containing 3D topological insulators are a rich platform for studying anomalous phase shifts and unconventional superconductivity [4,5]. Topological insulators have unique surface states which exhibit spin-momentum locking and preferentially transport supercurrents [6]. The surface properties, combined with strong spin-orbit coupling, enables phase manipulation beyond what is typically done in more conventional materials. Further, the interface between an s-wave superconductor and a 3D topological insulator is expected to host Majorana zero modes, particles that are their own antiparticle that follow non-Abelian statistics. Control over Majorana particles would enable the construction of highly fault-tolerant quantum

computers, but definitive detection of the particles is so far controversial. Because S-TI-S junctions are predicted to exhibit distinctive properties of Majorana modes [7] it is important to obtain a detailed understanding of the transport and phase signatures of different junction geometries and materials.

We study a junction made of Nb/Ti-Bi₂Se₃-Nb/Ti under conditions where applied magnetic fields, disorder, and spin-orbit coupling are expected to Josephson phase shifts. The primary measurements are magnetic diffraction patterns, or Fraunhofer interference patterns, which show a modulation of the critical current, and in turn the phase across the junction, as a function of the applied magnetic field. We observe asymmetry in the Fraunhofer patterns that does not show temperature dependence, and also find there are asymmetrical features for fields applied in the plane of the junction. Our main conclusion is that anomalous Fraunhofer features can manifest primarily from geometric effects, i.e. edge-steps and defects across the device. Understanding this is important in order to differentiate geometrical phase shifts from those caused Cooper pair momentum shifting, Majorana signatures, or other unconventional superconducting behavior.

Fraunhofer interference can be understood by considering a flat, rectangular junction where the flux penetrating perpendicular to the plane of the junction (the z-direction, as shown in Fig. 1a) causes a winding of the superconducting phase that leads to Equation 1 [8,9]:

$$I_c = I_{c,0} \left| \frac{\sin(\pi B A/\Phi_0)}{\pi B A/\Phi_0} \right| \tag{1}$$

Equation 1 shows that the critical current across the junction varies with the applied magnetic field, and the nodes in the critical current Fraunhofer pattern are located at $B = n\Phi_0/A$, where B is the applied magnetic field, A is the cross-sectional area of the junction, and $\Phi_0 = h/2e$ is the flux quantum. The nodes occur when an integer number of Φ/Φ_0 enter the junction.

The standard Fraunhofer pattern that follows the $\sin(\Phi)/\Phi$ form from Equation 1 can be modified in several ways, such as by the geometry of the sample [8,10], the temperature of the sample (through thermal cycling) [12], and as discussed above, by magnetic fields applied in-plane with the current. While behaviour that deviates from the standard Fraunhofer pattern has been documented and, in some cases, explained, all of the

mechanisms responsible for deviation are not completely understood. Features such as lifted nodes or suppressed lobes can be a result of multiple parameters, and simulations of these anomalous features sometimes rely on empirical methods, rather than a detailed theoretical understanding [3,9,13].

Other experiments on similar devices have shown an evolution of the critical current as a function of B_z consistent with a typical Fraunhofer pattern. But with an applied in-plane magnetic field parallel to the current, B_x , the Fraunhofer pattern develops side lobes that persist at higher B_x than the central lobe [10]. These side lobes can be caused by a Zeeman effect, which appears in the Hamiltonian of the surface states as [10,14,15]:

$$H = v_f \left(k_y - \frac{g\mu B_x}{\hbar v_f} \right) \sigma_y + \hbar v_f k_y \sigma_x \tag{2}.$$

In Equation 2, the momentum states k_y are translated by $g\mu B_x/hv_f$, which is known as a finite momentum shift of the Fermi surface. In the Hamiltonian, v_f is the Fermi velocity, g is the g-factor, and μ is the Bohr magneton. Each Cooper pair on the Dirac cone gets double this finite momentum shift, and so has a phase modulation $2g\mu xB_x/hv_f$ in the y-direction. Additionally, there may be an Aharonov-Bohm phase modulation, $\pi xB_y t/\Phi_0$ [10]. Thus, there is motivation to further understand the conditions under which momentum shifts are apparent in Fraunhofer patterns with applied in-plane magnetic fields, versus contributions from other effects (such as disorder or steps).

Equation 1 describes the Fraunhofer pattern for a rectangular, flat junction with only an out of plane magnetic field, and no screening effects [8], but asymmetries in the junction, in-plane magnetic fields, and magnetic domains in the junction can cause deviations from the standard pattern [3,10,16]. More specifically, as discussed earlier, an anomalous phase shift can arise from breaking sets of symmetries in the junction that change the relation, $I_c(+B_z) = I_c(-B_z)$ [3,13,15]. A strong spin-orbit coupling combined with an applied B_y is sufficient to produce an asymmetric Fraunhofer pattern, even within a geometrically symmetric junction. Tables of the operators that can break the symmetry of a Josephson junction are available in Ref. [3] and Ref. [15]. The important operator for this manuscript is V(x,y), as an asymmetric disorder potential by itself is enough to generate asymmetric Fraunhofer patterns. An asymmetric V(x,y)can exist because of asymmetric contact at the interface

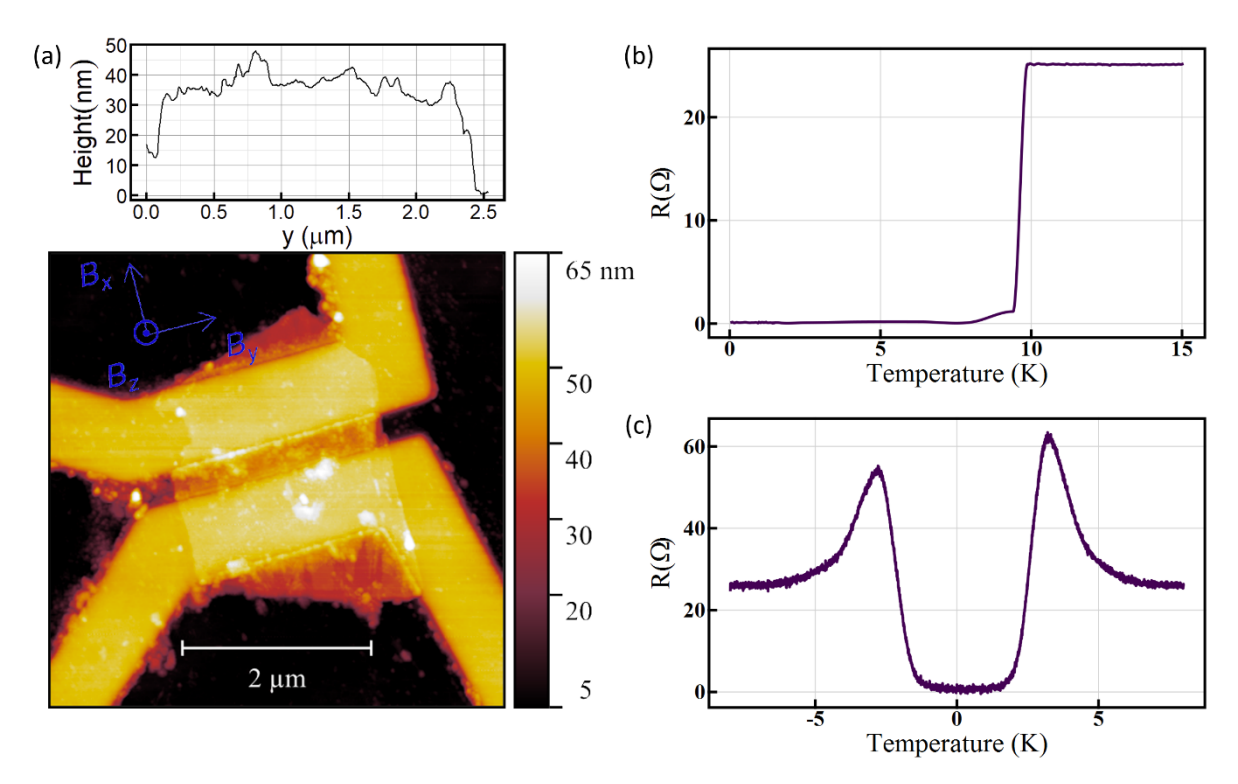


FIG. 1: (a) An AFM scan of the sample showing the flake (\sim 35 nm in height) and the quasi-four-point configuration of the leads, along with a height profile across the width of the flake. A large edge step is apparent in the height profile. (b) The resistance across the sample as a function of the temperature. NbTi is known to superconduct at \sim 9 K. (c) The dV/dI curve for the same sample, taken at 15 mK and zero magnetic field. The peaks at \pm 3 μ A delineate the critical current of the junction.

between the superconducting leads and the TI, because of geometrical asymmetry in the TI flake itself, or because of inconsistent current density across the TI. The following sections will show that microscopic disorder in the junction, arising from the TI flake itself, is enough to cause asymmetry and aperiodicity comparable to that generated by applied magnetic fields.

While Equation 1 holds true for an ideal junction in a perpendicular applied field, there is a more general way of writing the critical current of a Josephson junction, considering the size of the junction and an in-plane field:

$$I_{c} = \max_{\varphi'} \int_{-W/2}^{W/2} \int_{0}^{d} j_{0} \sin(\varphi_{xy}(y) + \varphi_{xz}(z) + \varphi' + \varphi_{0}(y)) dy dz$$
 (3).

Equation 3 expresses the critical current as a function of B_y and B_z , where W is the width of the junction in the y-direction, d is the thickness of the flake, j_0 is the critical current density, ϕ_{xy} is the flux produced by B_z which is proportional to yB_z , ϕ_{xz} is the flux produced by B_y , which is proportional to zB_y , φ' is a phase shift that is allowed to vary to maximize the critical current, and φ_0 is an anomalous phase shift that varies with y due to disorder in the junction [3]. Including y-dependence, of an

applied field or anomalous phase, in the calculation of the critical current allows for asymmetry. When φ_0 is constant, any changes it would make to the Fraunhofer pattern are cancelled out by the maximizing of φ' . However, if φ_0 varies with y, then the Fraunhofer pattern can show asymmetry, aperiodicity, and lifted nodes.

2. Experiment

Two devices were fabricated and measured, and showed similar behaviour, we present data from a single device that is representative of both. Figure 1a shows an AFM scan of the 2.26µm x 0.35µm junction, with a quasi-fourpoint lead design. Between the leads, the Bi₂Se₃ flake was ~ 35 nm thick, with 45 nm thick NbTi leads. NbTi was chosen for its relatively high critical field of ~ 9 T. The actual height of the sample at each point is important to the analysis in this paper, as a measure of geometric variations. At the top of Figure 1a is a height profile of the flake in the y-direction, where large steps and height variations show the variations in flake thickness. It is important to note that these thickness variations can cause anomalous features in magneto-transport

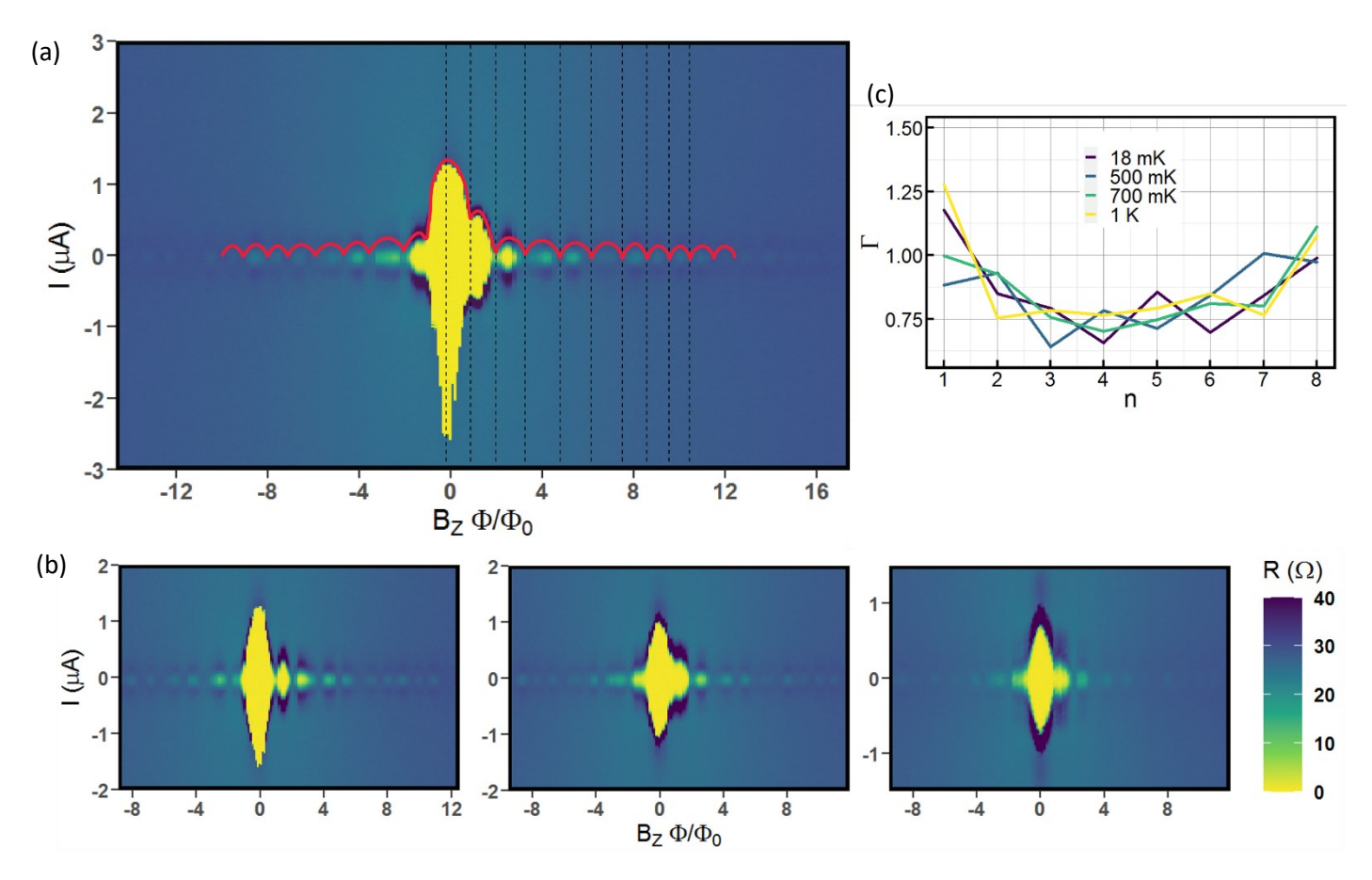


FIG. 2: (a) An asymmetric Fraunhofer pattern at 18 mK. The black dashed lines mark the positions of the first several nodes, while the red line roughly traces the critical current. (b) The Fraunhofer pattern at 500 mK (left), 700 mK (middle), and 1 K (right). (c) $\Gamma(B_{z,n})$ for each node, n, at all four temperatures.

measurements of the junction, including the asymmetry we present. All transport measurements were done in an Oxford Triton dilution refrigerator with temperature of 12 mK and a 6:1:1 T vector magnet, using a lock-in amplifier and DC-DAQ as current sources. The devices were made by mechanically exfoliating Bi₂Se₃ crystals with bulk carrier density, $n \sim 5 \times 10^{17} \text{cm}^{-3}$, onto Si having a 300 nm thick oxide layer. Candidate flakes were identified using an optical microscope and their thicknesses were verified via AFM. We targeted a thickness of 20 nm to 40 nm, to yield junctions thin enough to have limited bulk conduction but thick enough to avoid hybridization effects.

3. Results

Both devices were first measured to confirm that the leads and Bi_2Se_3 superconduct at low temperatures. Figures 1b and c show that the representative junction superconducts at a critical temperature of ~ 9 K, and has

a critical current of $\sim 3~\mu A$, measured at 5 mK. The normal state resistance of the junction is 25 Ω , giving $I_cRNe=0.075~\text{meV}$, while the expected gap energy of the leads is, $\Delta=3.05~\text{meV}$ [17,18]. These values agree with what is expected for S-TI-S junctions [9].

The measured area of the junction in the x-y plane is given by the junction length and the width of the sample between the leads: $2.26~\mu m \times 0.35~\mu m = 0.79~\mu m^2$. However, flux focusing increases the effective area of the junction to $2.2~\mu m^2$. Flux focusing occurs when magnetic field lines that would have penetrated the leads are diverted to the closest non-Meissner state area, which means more magnetic field lines are penetrating the TI flake than would be if the leads were not a superconducting material. Additionally, there is some penetration depth of the magnetic field into the leads, increasing the effective area by adding $2\lambda L$ to the distance between the leads. The effective area due to flux focusing, $2.2~\mu m^2$, agrees well with an estimation done

by fitting the first few nodes of the Fraunhofer patterns in Figure 2.

Figures 2a and 2b show Fraunhofer patterns for the device at T = 18mK, 500mK, 700mK, and 1K. Using the effective area, the plot axes in Figures 2a and 2b are converted from Tesla to units of flux divided by the flux quantum, in order to compare the measured pattern with Equation 1. The yellow superconducting regions should be symmetric in spacing and intensity, according to Eq. 1. However, it is clear in the Figure that for all temperatures, the patterns are asymmetric in node spacing as well as in intensity for $+B_z$ and $-B_z$. The spacing of the nodes is not significantly changed by the temperature, but higher temperatures do lower the amplitude of the pattern and washout the higher field features. From Equation 1, the nodes in the Fraunhofer pattern are expected at $B_z = n\Phi_0/A$, i.e. when integer number of flux quanta enter the junction. If A in Equation 1 is the effective area due to flux focusing, the observed node spacing in Figures 2a and 2b only roughly agrees with the spacing expected from Equation 1. The trace of I_c for the 18 mK measurement shows the shape of the nodes and antinodes, and examination of the distance from each node to the next (dotted black lines in Fig. 2), makes it clear that the spacing for the first few nodes and antinodes is aperiodic, which is not predicted by Equation 1. The deviation factor, $\Gamma(B_{z,n}) =$ $n\Phi_0/B_{z,n}A_{eff}$, captures the observed difference between the expected position of the n-th node and the actual position, and is plotted in Figure 2c. In Figure 2c we see that as B_z increases, Γ has a concave shape, approaching unity for nodes at higher field values. In other words, the deviation disappears at large field values, but is significant ($\Gamma \sim 0.7$) elsewhere, with the first node especially different from the 3rd, 4th, and 5th. It can also be seen that the overall shape of Γ is not affected by the temperature of the sample.

Aperiodic spacing of Fraunhofer lobes has been observed before in Al-TI-Al junctions [9,17]. One phenomenological explanation given for this data argues that as the applied field increases, the superconducting leads transition from a Meissner state to a state with vortices, resulting in less flux being redirected into the sample. Consequently, at higher fields, the effective area of the junction is smaller, and the nodes are spaced farther apart [13]. However, we observe that as the magnetic field increases, the nodes of the Fraunhofer patterns in Figures 2a and 2b become more closely spaced together, which is inconsistent with the

weakened flux focusing picture. It has also been observed that an S-TI-S junction can become SQUID-like with a non-uniform current density [19] or with sufficient B_x [13]. However, we observe that this form of aperiodicity exists at $B_x = 0$ and $B_y = 0$, which rules out the B_x -SQUID picture. Thus, the aperiodic node spacing we observe is likely the result of non-uniform current density caused by the geometry of the flake itself, e.g. voltage drops that occur at atomic steps in the TI, such as those that can be seen in Figure 1a.

The amplitude of the Fraunhofer lobes deviates from the expected symmetry as well. Amplitude asymmetry can be thought of as arising from a skip in the phase difference in the plane of the junction, with the skip generated by an in-plane magnetic field [19]. Additionally, a varying flake thickness changes the value of the Rashba coefficient and can produce asymmetry in the Fraunhofer patterns via phase skipping [3]. It is possible the trapped flux or flux focusing effects could create a finite in-plane magnetic field that would cause an amplitude asymmetry at no applied field bias [13,20,21]. To test this, in Figure 3 we show how the Fraunhofer patterns vary with in-plane magnetic fields. The Figure shows that asymmetries in node spacing and amplitude exist for all values and both directions of inplane fields. A possible explanation for this is that the current density in the junction is anisotropic. Because there is not a value of B_x or B_y that produces a pattern symmetric in B_z , the asymmetries cannot be due to the creation of in-plane magnetic fields. An asymmetry in the superconducting contacts of a Josephson Junction has also been shown to lead to asymmetric Fraunhofer patterns [3,10], but the ratio of the widths of our contacts, $\alpha = W_1/W_2 = 1.02$, is close enough to 1 that it is unlikely to cause such a large asymmetry when compared to calculations. Consequently, it is likely that both the asymmetry and aperiodicity of the B_z vs. I Fraunhofer patterns is primarily due to steps in the flake

Equation 1 predicts that the Fraunhofer amplitude decays like 1/B about B=0, but an additional B_x magnetic field along the direction of the current will transfer amplitude from the central lobe to side lobes [3]. The junction in this experiment is fabricated similarly to the samples in Ref. [10], but shows a much less pronounced raising of the side lobes than those devices. The same experiment shows via simulations that samples with a large bulk transport carrier density will have greatly reduced side branches, because the bulk

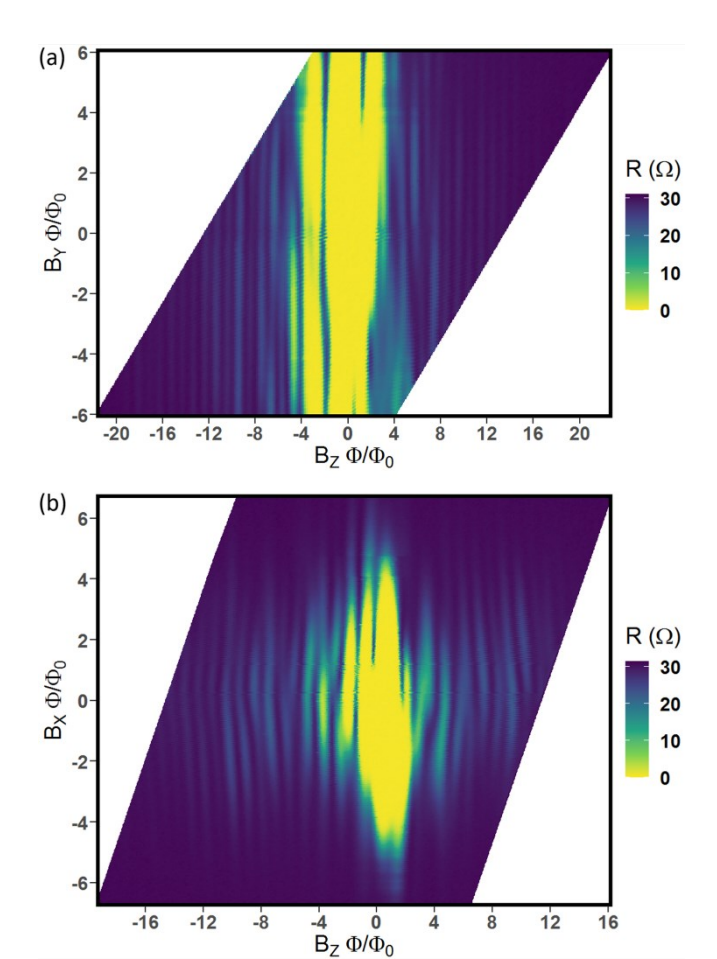


FIG. 3: B_z vs B_x (a), and B_z vs B_y (b), both plots have been rotated so that the lobes are vertical. The maps show an asymmetrical resistance pattern at all values of B_x and B_y .

carriers do not pick up a significant Aharanov-Bohm phase. Thus, the current experiment may be in a highcarrier density regime where side lobe branches are suppressed.

As a comparison to our data, in Fig. 4a we show a plot of a Fraunhofer pattern generated from Equation 3 and utilizing the $\varphi_0(y)$ shown in Fig. 4b, which has an explicit phase jump. The Fraunhofer pattern in Figure 4 comes directly from numerically integrating Equation 3, and choosing W = 2, d = 1, and $j_0 = 0.5$, to create an easily readable, unitless scale. φ_0 is set to the linear form shown in Fig. 4b, where φ_{xy} and φ_{xz} are geometric functions of the magnetic field, and we let $B_y = 0$ to get a 1D slice. Fig. 4a shows that a linear $\varphi_0(y)$ with a single phase jump can generate asymmetry, aperiodicity, and lifted nodes. A phase jump like this could be caused by a height jump, or disorder potential in the junction, like what we observe in our Bi₂Se₃ flake.

It has also been reported that in Josephson junctions with inversion symmetry-breaking weak links there can be an asymmetry in the Fraunhofer patterns that depends on the current direction, $|I_c^+(B)| \neq |I_c^-(B)|$, as well as asymmetry that depends on the applied field direction, $|I_c^\pm(B)| \neq |I_c^\pm(-B)|$ [22]. It is possible that this inversion-symmetry breaking contributes to the asymmetry observed in our Fraunhofer patterns; however, we do not observe the mirror symmetry expected in this case, indicating that disorder effects may dominate in our devices.

4. Conclusion

An S-TI-S junction fabricated from NbTi and Bi₂Se₃ shows an asymmetric Fraunhofer pattern at zero in-plane field, which persists from <15 mK to >1 K. We observe additional asymmetry due to an applied B_y in the plane of the junction, but perpendicular to the direction of the current, which shifts amplitude from one polarity of the Fraunhofer pattern to the other. The measurements of amplitude asymmetry in both the B_x and B_y directions

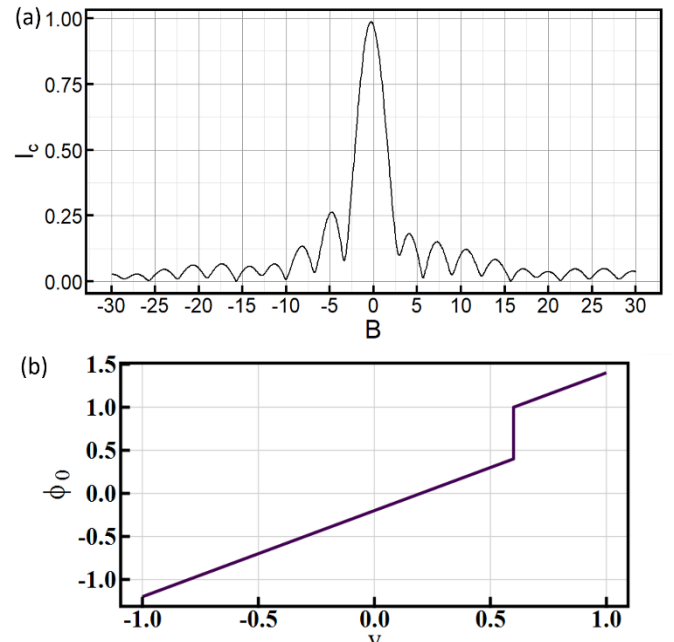


FIG. 4: (a) A Fraunhofer pattern generated using Equation 3 and the $\varphi_0(y)$ shown below, with $B_y = 0$. The pattern demonstrates amplitude asymmetry, aperiodicity, and lifted nodes. The critical current is normalized to 1 and the magnetic field has arbitrary units. b) The $\varphi_0(y)$ used in Equation 3 to generate the Fraunhofer pattern above, where y is an arbitrary unit of distance, and ranges from one edge of the junction to the other.

point to a current density origin of these effects, caused by edge-stepping or other disorder effects in the TI. Finally, we observe aperiodic spacing of the Fraunhofer lobes/nodes that is contrary to previously observed behaviour that was attributed to weakened flux focusing effects. Our observation that the spacing rises for the first few nodes, then falls towards a regular pattern suggests a more complicated, geometry dependent critical current-flux relationship [8,19,24,25]. To probe the strength of these effects further, it will be useful to fabricate junctions with intentionally symmetry breaking properties, that are expected to dominate the anomalous features of the critical current and Fraunhofer patterns.

References

- [1] Kockum, A., and Nori, F. 2019. Quantum Bits with Josephson Junctions. *Springer Series in Materials Science*, p.703–741.
- [2] Bergeret, F., and Tokatly, I. 2015. Theory of diffusive Josephson junctions in the presence of spin-orbit coupling. *EPL*, 110(5), p.57005.
- [3] Assouline, A., Feuillet-Palma, C., Bergeal, N., Zhang, T., Mottaghizadeh, A., Zimmers, A., Lhuillier, E., Eddrie, M., Atkinson, P., Aprili, M., and Aubin, H. 2019. Spin-Orbit induced phase-shift in Bi₂Se₃ Josephson junctions. *Nature Communications*, 10(1), p.126.
- [4] Likharev, K. 1979. Superconducting weak links. *Rev. Mod. Phys.*, *51*, p.101–159.
- [5] Sato, M., and Ando, Y. 2017. Topological superconductors: a review. *Reports on Progress in Physics*, 80(7), p.076501.
- [6] Cho, N. 2013. Symmetry protected Josephson supercurrents in three-dimensional topological insulators. *Nature Communications*, *4*(1), p.1689.
- [7] Hasan, M., and Kane, C. 2010. Colloquium: Topological insulators. *Rev. Mod. Phys.*, 82, p.3045–3067.
- [8] Tinkham, M. 2004. *Introduction to Superconductivity*. Dover Publications.
- [9] Williams, J., Bestwick, A., Gallagher, P., Hong, S., Cui, Y., Bleich, A., Analytis, J., Fisher, I., and

- Goldhaber-Gordon, D. 2012. Unconventional Josephson Effect in Hybrid Superconductor-Topological Insulator Devices. *Physical Review Letters*, 109(5).
- [10] Chen, A., Park, M., Gill, S., Xiao, Y., Reig-i-Plessis, D., MacDougall, G., Gilbert, M., and Mason, N. 2018. Finite momentum Cooper pairing in three-dimensional topological insulator Josephson junctions. *Nature Communications*, *9*(1), p.3478.
- [11] Galletti, L., Charpentier, S., Iavarone, M., Lucignano, P., Massarotti, D., Arpaia, R., Suzuki, Y., Kadowaki, K., Bauch, T., Tagliacozzo, A., Tafuri, F., and Lombardi, F. 2014. Influence of topological edge states on the properties of Al/Bi₂Se₃/Al hybrid Josephson devices. *Phys. Rev. B*, 89, p.134512.
- [12] Schuffelgen P. et al. 2017. Boosting Transparency in Topological Josephson Junctions via Stencil Lithography. *arXiv: Superconductivity*.
- [13] Suominen, H., Danon, J., Kjaergaard, M., Flensberg, K., Shabani, J., Palmstrom, C., Nichele, F., and Marcus, C. 2017. Anomalous Fraunhofer interference in epitaxial superconductor-semiconductor Josephson junctions. *Phys. Rev. B*, *95*, p.035307.
- [14] Zhang, H., Liu, C.X., Qi, X.L., Dai, X., Fang, Z., and Zhang, S.C. 2009. Topological insulators in Bi₂Se₃, Bi₂Te₃ and Sb₂Te₃ with a single Dirac cone on the surface. *Nature Physics*, 5(6), p.438–442.
- [15] Rasmussen, A., Danon, J., Suominen, H., Nichele, F., Kjaergaard, M., and Flensberg, K. 2016. Effects of spin-orbit coupling and spatial symmetries on the Josephson current in SNS junctions. *Physical Review B*, 93(15).
- [16] Börcsök, B., Komori, S., Buzdin, A., and Robinson, J. 2019. Fraunhofer patterns in magnetic Josephson junctions with non-uniform magnetic susceptibility. *Scientific Reports*, *9*(1), p.5616.
- [17] Kittel, C. 2004. *Introduction to Solid State Physics*. Wiley.
- [18] Moreland, J., Ekin, J., and Goodrich, L. 1986. Electron Tunneling into Superconducting Filaments: Depth Profiling The Energy GAP of NbTi Filaments from Magnet Wires. Springer.

- [19] Lee, J., Lee, G.H., Park, J., Lee, J., Nam, S.G., Shin, Y.S., Kim, J., and Lee, H.J. 2014. Local and Nonlocal Fraunhofer-like Pattern from an Edge-Stepped Topological Surface Josephson Current Distribution. *Nano Letters*, *14*(9), p.5029-5034.
- [20] Mayer, W., Dartiailh, M., Yuan, J., Wickramasinghe, K., Rossi, E., and Shabani, J. 2020. Gate controlled anomalous phase shift in Al/InAs Josephson junctions. *Nature Communications*, 11(1), p[21].2.
- [21] Kayyalha, M., Kazakov, A., Miotkowski, I., Khlebnikov, S., Rokhinson, L., and Chen, Y. 2018. Highly skewed current-phase relation in superconductor-topological insulator-superconductor Josephson junctions. *arXiv*.
- [22] Chen, C.Z., He, J., Ali, M., Lee, G.H., Fong, K., and Law, K. 2018. Asymmetric Josephson effect in inversion symmetry breaking topological materials. *Phys. Rev. B*, *98*, p.075430.
- [23] Bocquillon, L. 2017. Gapless Andreev bound states in the quantum spin Hall insulator HgTe. *Nature Nanotechnology*, *12*(2), p.137-143.
- [24] Antonio Barone, and Gianfranco Paternò 2005. "Small" Junctions in a Magnetic Field. John Wiley & Sons, Ltd.
- [25] Charpentier S. et al. 2017. Induced unconventional superconductivity on the surface states of Bi₂Te₃ topological insulator. *Nature Communications*, 8.